Table III. ^{13}C NMR Chemical Shifts of Homoadamantane Derivatives

compd	chemical shift/ppm[a]										
	C-1	C-2	C-3	C-4	C-5	C-6	C-7	C-8	C-9	C-10	C-11
4	27.5	38.2	31.8	33.8	33.8	31.8	38.2	27.5	36.3	38.2	38.2
7[b]	26.5*	29.7	37.6	88.3	41.5	29.0	39.5	26.7*	35.4†	35.8†	34.9
8a[c]	26.8*	29.8	34.9	86.1	41.8	29.4	40.0	27.3*	35.9†	36.5†	35.9
8b[d]	26.9*	30.4	36.7	78.9	41.0	29.4	39.8	27.0*	35.6†	36.1†	35.4
8c[e]	26.9*	29.6	35.6	86.5	41.4	29.3	39.8	27.2*	35.6†	36.3†	35.8
9c[f]	30.7*	87.3	36.1	29.1	33.2†	30.4*	39.0§	26.7	29.1	33.1§	32.8†
10	29.8	33.9	32.3	138.0	138.0	32.3	33.9	29.8	37.0	33.9	33.9
11	21.2	12.6	10.0	10.0	28.3	26.4	38.6	26.4	32.2	32.2	28.3

[a] Measured at 67.8 MHz in $CDCl_3$. The ring carbons are numbered as indicated in eq 1. Chemical shifts marked with *, †, and § may be interchanged. [b] Tosylate group: 144.2, 134.7, 129.6, 127.5, and 21.5 ppm. [c] Methoxy group: 56.3 ppm. [d] Acetyl group: 170.0 and 21.3 ppm. [e] Trifluoroethyl group: 124.2 and 66.3 ppm. [f] Trifluoroethyl group: 124.3 and 66.3 ppm.

Table IV. ^{13}C Distributions in the 4-Substituted Homoadamantanes (8a-c)[a] and *exo*-2-(Trifluoroethoxy)homoadamantane (9c) from the Solvolysis of [3-^{13}C]-7

solvent	product	^{13}C distribution[b] (%)										
		C-1	C-2	C-3	C-4	C-5	C-6	C-7	C-8	C-9	C-10	C-11
MeOH	8a	0.2*	0.4	54.7	43.9	0.4	0.4	0.0	0.0*	0.0	0.0	0.0
AcOH	8b	1.0*	0.9	49.2	44.4	1.8	1.8	0.0	0.5*	0.1†	0.0†	0.3
TFE	8c	1.5*	1.5	46.6[c]	45.6	1.6	1.6	0.0	0.6*		0.2[d]	0.8
TFE	9c	0.4*	0.4	47.8	46.0[e]	1.6†	1.6*	0.0	1.2		0.0	1.0†

[a] The ring carbons of 8a-c are numbered as indicated in eq 1. [b] Numbers marked with * and † may be interchanged. [c] C-3 + (C-9 or C-10). [d] C-9 or C-10. [e] C-4 + C-9.

Table V. ^{13}C Distributions in the 4-Homoadamantane (10) from the Solvolysis of [3-^{13}C]-7

solvent	^{13}C distribution (%) in 10				
	C-1,8	C-2,7,10,11	C-3,6	C-4,5	C-9
MeOH	0.1	0.0	62.3	37.6	0.0
AcOH	0.8	0.6	56.8	41.8	0.0
TFE	1.2	0.8	55.4	42.4	0.2

more shielded than the former owing to the oxygen atom attached to C-4.[9] The assignments of C-1 and C-8 and those of C-9 and C-10, however, remained interchangeable with this procedure. The spectrum of **9c** was analyzed in the same way, but the assignments were only partially successful. The signals of **10** and **11** obtained from the labeled tosylate were assigned unambiguously with the assumption that the label was located mainly at C-3 and C-4.

For the determination of label distribution, proton-decoupled ^{13}C NMR spectra were measured in the presence of a relaxation reagent $Fe(acac)_3$[10] (0.05 M) by the gated decoupling method. The ^{13}C content at the nth carbon (x_n, n = 1–11) was calculated from peak integrations (A_n) by the following equation.

$$x_n\,(\%) = (96.8 + 10(1.108))A_n/\sum A_n \qquad (2)$$

To obtain label distribution, these values were subtracted by the natural abundance of ^{13}C (1.108%) and normalized in such a way that the total is 100%. The resulting data are given in Tables IV–VI. Generally, uncertainty limit for the label percent is estimated to be ±0.5% at C-3 and C-4 and ±0.2% at other positions. In the case of 2,4-dehydrohomoadamantane (**11**), however, greater errors were observed for some carbons (Table VI), owing to significant overlap of signals. Yields of **9a** and **9b** were so low that the low singal-to-noise ratios did not allow integrations with sufficient precision.

(9) Duddeck, H.; Wolff, P. *Org. Magn. Reson.* **1977**, *9*, 528.
(10) Martin, M. L.; Martin, G. J.; Delpuech, J.-J. *Practical NMR Spectroscopy*, Heyden and Sons: London, 1980; Chapter 10, Section 3.

Table VI. ^{13}C Distributions in the 2,4-Dehydrohomoadamantane (11)[a] from the Solvolysis of [3-^{13}C]-7

solvent	^{13}C distribution (%) in 11						
	C-1	C-2	C-3,4	C-5,11	C-6,8	C-7	C-9,10
MeOH	0.0	0.1	98.7	0.2	0.4	0.0	0.6 ± 1.0
AcOH	0.2	0.1	93.8	1.8	2.4	0.0	1.7 ± 1.0
TFE	1.0	0.7	93.5	1.9	1.6	0.8	0.5 ± 1.0

[a] The ring carbons of 11 are numbered as indicated in eq 1.

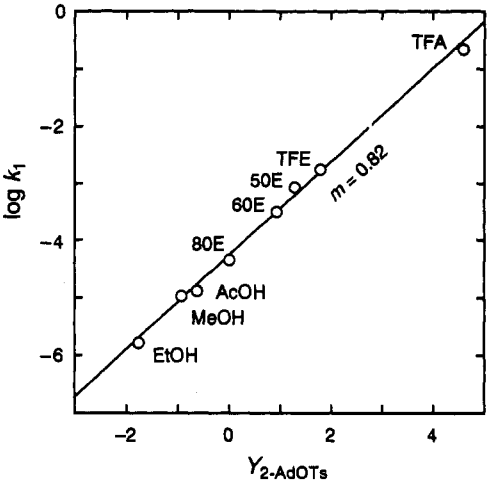

Figure 1. Plot of log k_1 for solvolysis of 4-homoadamantyl tosylate at 25 °C vs $Y_{2\text{-AdOTs}}$.

Discussion

Solvent Effect on Solvolysis Rates. A plot of log k_1 at 25 °C against $Y_{2\text{-AdOTs}}$ of the solvent showed a linear correlation with a slope of 0.82 (Figure 1, r = 0.998). The linear plot over a wide range of solvent ionizing power with a slope close to unity indicates that 4-homoadamantyl tosylate practically undergoes a limiting k_c process. This result supports the previous conclusion given by Nordlander[4] that the 4-homoadamantyl tosylate is highly resistant to backside nucleophilic assistance by solvent

Scheme I

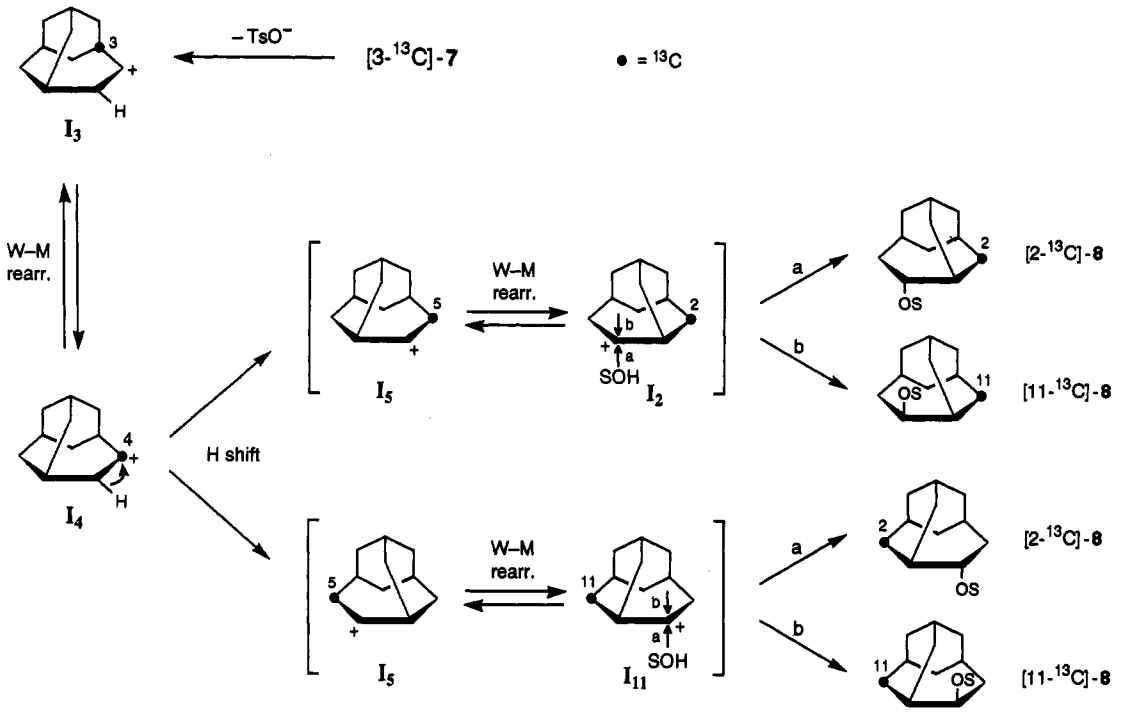

owing to steric limitations similar to those observed for the solvolysis of the 2-adamantyl systems.

Structure of 4-Homoadamantyl Cation. The result of the label analysis for the 4-substituted products, 8a-c (Table IV), provided detailed information on the structure and the reactivity of the 4-homoadamantyl cation intermediate.

The unequal label distributions on C-3 and C-4 indicate that the 3,4-methylene shift equilibrium is not completely established prior to product formation. The observed ratios of 3-^{13}C/4-^{13}C, 1.25 ± 0.03 (MeOH), 1.11 ± 0.02 (AcOH), and 1.02 ± 0.02 (TFE), show distinct deviation from those expected from primary carbon-13 isotope effect on the carbenium ion stability. Saunders et al.[11] have reported that 2,3-dimethyl[2-^{13}C]-2-butyl cation in SbF_5/SO_2ClF favors the positive charge on the labeled carbon with equilibrium constants ($^{12}C^+/^{13}C^+$) ranging between 0.9840 (-108 °C) and 0.9884 (-61 °C). A similar isotope effect, $^{12}C^+/^{13}C^+$ = 0.9833, has been reported by Kresge et al.[12] for ionization of triphenyl[^{13}C]methyl chloride in SO_2 at 0 °C.

The greater extent of C-3–C-4 scrambling in a less nucleophilic solvent is taken as evidence against the symmetrical, σ-bridged structure and is interpreted as indicating that the 4-homoadamantyl cation is a classical ion that is rapidly rearranging via the degenerate Wagner–Meerwein process. The contribution of nucleophilic solvent assistance is considered unlikely, based on the result of the rate study, as well as on the greater extent of C-3–C-4 label scrambling in substitution than in elimination (*vide infra*).

More convincing evidence for the classical nature of 4-homoadamantyl cation is provided by inspecting the 4-substituted homoadamantanes (8a-c) produced from unsymmetrically labeled intermediates, e.g., [2-^{13}C]- and [11-^{13}C]-4-homoadamantyl cations (I_2 and I_{11}, the subscript represents the position of the label[13]), which are potential precursors of both [2-^{13}C]-8 and [11-^{13}C]-8 (Scheme I). If these cations had σ-bridged structures I_5

$I_5 \leftrightarrow I_2$ $I_5 \leftrightarrow I_{11}$

$\leftrightarrow I_2$ and $I_5 \leftrightarrow I_{11}$, respectively, attack of the solvent molecule from the frontside of the bridge would be strictly prohibited. This should result in exclusive formation of [2-^{13}C]-8 rather than [11-^{13}C]-8. Therefore, the observed formation of a significant amount of [11-^{13}C]-8 (2-^{13}C: 11-^{13}C ≃ 2:1, Table IV) is strong evidence for the absence of σ-bridging. This conclusion is in accord with the absence of cis–trans stereospecificity in the 5,4-hydride shift of the 4-homoadamantyl cation reported by Nordlander.[4] Since the equilibrating ions $I_5 \rightleftarrows I_2$ and $I_5 \rightleftarrows I_{11}$ are supposed to have lost contact relationship with the tosylate anion after the preceding hydride shift,[4] the steric effect by the counterion may not be the source of the stereoselectivity. The preferred formation of [2-^{13}C]-8 is rather ascribed to the steric inhibition of the solvent attack from the direction cis to the migrating carbon.

These results are in contrast to that reported for bicyclo[3.2.1]oct-2-yl cation. Goering[14] proposed a σ-bridged structure 12 based on the fact that acetolysis of *endo*-bicyclo[3.2.1]oct-2-yl tosylate proceeds with complete retention of configuration. Appropriate orbital overlap for a symmetrically bridged structure appears much more encumbered in the homoadamantyl cation (2) than in 12, although both cations are analogous in that positively charged carbons belong to a seven-membered ring. A similar geometric restriction has been suggested by Ber-

(11) Saunders, M.; Cline, G. W. *J. Am. Chem. Soc.* **1990**, *112*, 3955.
(12) Kresge, A. J.; Lichtin, N. N.; Rao, K. N.; Weston, R. E., Jr. *J. Am. Chem. Soc.* **1965**, *87*, 437.
(13) The ring carbons of the 4-homoadamantyl cation are numbered as indicated in structural formula 1.
(14) Goering, H. L.; Sloan, M. F. *J. Am. Chem. Soc.* **1961**, *83*, 1397.

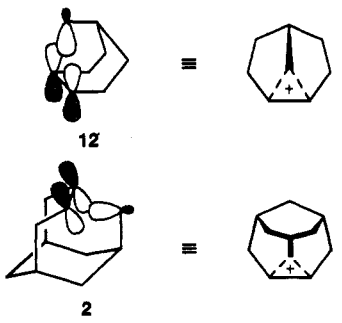

12 2

son[15] for the bicyclo[3.2.2]non-2-yl cation to explain the difficulty in attaining a σ-bridged structure.

Relative Rates of Wagner–Meerwein Rearrangement and Vicinal Hydride Shift. If the absence of frontside–backside stereospecificity with respect to the leaving group is assumed for both methylene and hydride migration, a diagram involving all the possible transformations among labeled 4-homoadamantyl cations $\mathbf{I}_n$ (n = 1–11) can be drawn as Scheme II.

The major distribution of the label at C-3 and C-4, but not at C-3 and C-6, with approximately equal populations clearly demonstrates predominant Wagner–Meerwein rearrangement (k_w) over 5,4-hydride shift (k_h). The formation of 4-substituted products **8a-c** labeled at positions other than C-3 or C-4 requires at least one hydride shift. The low total yields of such products, 1.4% (MeOH), 6.4% (AcOH),[16] and 7.8% (TFE), reflect the sluggishness of hydride shift compared to product formation. In particular, the negligible yields of **8a-c** labeled at C-7, -9, and -10, for which a second hydride shift is required, indicate that only the first hydride shift is significant. Further hydride shifts can then be ignored, thereby allowing simplification of the mechanistic model as illustrated in Scheme III.[17] $\mathbf{R}_n$ and $\mathbf{P}_n$ represent, respectively, the tosylate **7** and the 4-substituted product **8** labeled at the nth carbon. Rate constants k_i, k_{-i}, and k_p correspond to ionization, ion pair return, and product formation, respectively.

Steady-state treatment with respect to $\mathbf{I}_3$ and $\mathbf{I}_4$ results in the following rate expressions for tosylate consumption and product distribution

$$[\mathbf{R}_3] + [\mathbf{R}_4] = C_0 \exp\left(-\frac{k_i(k_p + k_h)}{k_{-i} + k_p + k_h}t\right) \quad (3)$$

$$[\mathbf{R}_3] - [\mathbf{R}_4] = C_0 \exp\left(-\frac{k_i(k_p + 2k_w + k_h)}{k_{-i} + k_p + 2k_w + k_h}t\right) \quad (4)$$

$$([\mathbf{P}_3] + [\mathbf{P}_4])_{t=\infty} = \frac{k_p}{k_p + k_h}C_0 \quad (5)$$

$$([\mathbf{P}_3] - [\mathbf{P}_4])_{t=\infty} = \frac{k_p}{k_p + 2k_w + k_h}C_0 \quad (6)$$

where C_0 is the initial concentration of the substrate [3-^{13}C]-**7**. Equations 5 and 6 afford expressions for the rates of Wagner–Meerwein rearrangement and vicinal hydride shift relative to solvent capture:

$$k_h/k_p = C_0/([\mathbf{P}_3] + [\mathbf{P}_4])_{t=\infty} - 1 \quad (7)$$

$$k_w/k_p = 0.5[C_0/([\mathbf{P}_3] - [\mathbf{P}_4])_{t=\infty} - (k_h/k_p) - 1] \quad (8)$$

From the fraction of **8a-c** labeled at C-3 and C-4 (Table IV), values for these rate ratios were calculated as listed in Table VII. This result allows evaluation of the rate of Wagner–Meerwein rearrangement relative to vicinal hydride shift: k_w/k_h = 340 ± 140 (MeOH), 140 ± 20 (AcOH), and 760 ± 340 (TFE).[18]

Ion Pair Return. The rates of ionization (k_i) and ion pair return (k_{-i}) in eqs 3 and 4 are related to two phenomenological rate constants, k_1 and k_{sc}.

$$k_1 = \frac{k_i(k_p + k_h)}{k_{-i} + k_p + k_h} \quad (9)$$

$$k_{sc} = \frac{k_i(k_p + 2k_w + k_h)}{k_{-i} + k_p + 2k_w + k_h} \quad (10)$$

The rate of tosylate scrambling, k_{sc}, can be derived from eq 4 using the data from acetolysis of [3-^{13}C]-**7** over 1.0 half-life (141 min). The recovered tosylate had retained 54.1 ± 0.5% label at C-3, and 44.1 ± 0.5% of the label was found at C-4. This result, which corresponds to k_{sc} = (2.72 ± 0.06) × 10^{-4} s^{-1}, indicates involvement of appreciable ion pair return through the Wagner–Meerwein process.

With this value for k_{sc} and the values for k_1, k_w/k_p, and k_h/k_p (Tables I and VII), eqs 9 and 10 are solved simultaneously with respect to k_1 and k_{-i}/k_p, yielding k_i = 3.1 × 10^{-4} s^{-1} and k_{-i}/k_p = 3.0. The fractional conversion

Scheme II

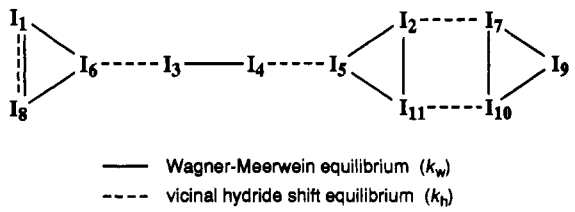

Scheme III

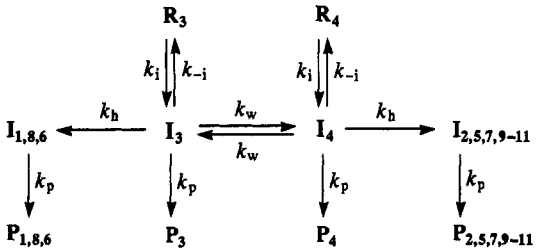

Table VII. Rate Constants of the Wagner–Meerwein Rearrangement (k_w) and 5,4-Hydride Shift (k_h) Relative to Solvent Capture (k_p) for the 4-Homoadamantyl Cation at 40 °C

solvent	k_w/k_p[a]	k_h/k_p
MeOH	4.1 ± 0.2	0.014 ± 0.005
AcOH	9.7 ± 0.8	0.068 ± 0.006
TFE	66 ± 33	0.085 ± 0.006

[a] See ref 18.

(15) Berson, J. A.; Luibrand, R. T.; Kundu, N. G.; Morris, D. G. *J. Am. Chem. Soc.* **1971**, *93*, 3075.

(16) Nordlander[4] reported that 18.6% of **8b** was formed with hydride shift in the acetolysis of [4-^{2}H]-**7**. As he pointed out, however, this number is an overestimation due to a large isotope effect by deuterium.

(17) The rate constant k_h as defined by Scheme III corresponds to half of that used in the kinetic treatment by Nordlander.[4]

(18) The errors in k_w/k_p and k_w/k_h are relatively large for TFE, since the small difference between $[\mathbf{P}_3]$ and $[\mathbf{P}_4]$ is amplified in eq 8.

of intermediates to products is $k_1/k_i = 0.26$, which is in good agreement with the result (0.30) derived from the deuterium scrambling of [4-^{2}H]-**7** under the same conditions.[4] The combined data from 1.0 and 20 half-lives provide the relative rates of the four competitive processes concerning the fate of 4-homoadamantyl cation in AcOH at 40 °C: $k_p:k_{-i}:k_w:k_h = 1:3.0:9.7:0.068$. Thus, an unprecedentedly detailed picture of the reactivity was obtained for a secondary alicyclic carbenium ion that is degenerate with respect to both Wagner–Meerwein rearrangement and 1,2-type hydride shifts.

Mechanism of 4,5-Elimination. Nordlander has reported that the acetolytic elimination of 4-homoadamantyl tosylate to produce 4-homoadamantene (**10**) takes place by a syn E1 mechanism in which the effective base is tightly paired tosylate anion.[4] The basicity of the tosylate ion is reduced in a highly ionizing solvent by electrophilic solvation. This accounts for the substantial decrease in the yield of 4-homoadamantene with increasing ionizing power of the solvent (Table II). Similar dependence of elimination/substitution ratio on solvent ionizing power has been observed for the solvolysis of cyclooctyl brosylate.[19]

The ^{13}C label distribution analysis for 4-homoadamantene provided further evidence for the above mechanistic view. First, if elimination is to occur in an earlier ion-pair stage than substitution, a relatively low degree of Wagner–Meerwein equilibration would be attained during the course of 4-homoadamantene formation. Although direct measurement of the label distributions on C-3 and C-4 was not possible owing to the symmetry of the 4-homoadamantene molecule, the ratios C-3,6/C-4,5 = 1.66 ± 0.04 (MeOH), 1.36 ± 0.03 (AcOH), and 1.31 ± 0.03 (TFE) may be good approximations to the extent of C-3–C-4 label scrambling. As expected, comparison of these values with those observed for the 4-substituted products, 1.24 ± 0.03 (MeOH), 1.10 ± 0.02 (AcOH), 1.02 ± 0.02 (TFE), clearly indicates the more limited scrambling in elimination. Secondly, the sum of the label distributions at positions other than C-3, -4, -5, and -6 is a measure of the degree of 5,4-hydride shift: the values 0.1% (MeOH), 1.4% (AcOH), and 2.2% (TFE) were observed for 4-homoadamantene, which are significantly smaller than those observed for 4-substituted products, 0.6% (MeOH), 2.8% (AcOH), and 4.6% (TFE). This finding indicates a smaller degree of 5,4-hydride shift in elimination, and further supports the earlier formation of the olefin relative to the substitution product.

2,4-Hydride Shift. Nordlander et al. have obtained 4-homoadamantyl trifluoroacetate (**8d**) and *exo*-2-homoadamantyl trifluoroacetate (**9d**) in 72% and 28% yields, respectively, from the trifluoroacetolysis of 4-homoadamantyl tosylate.[4] They pointed out the possibility that the 2,4-hydride migration occurs within a σ-bridged cation **2**, which is formed as a second-stage intermediate from localized 4-homoadamantyl cation. Our results, however, indicated a different mechanistic possibility. If the *exo*-2-substituted products **9a-c** were produced via a symmetrically bridged cation **2**, the C-3/C-4 label distribution ratios should be 1 (or smaller if primary ^{13}C isotope effect is taken into account, *vide supra*). The observed ratio for **9c** was 1.04 ± 0.02 (or greater owing to the overlap of C-4 and C-9 signals, Table IV), which is comparable to that observed for **8c** (1.02 ± 0.02). This result suggests that **9c** was formed through direct 2,4-hydride migration from localized 4-homoadamantyl cation.

The fact that the yields of **9a-d** (Table II) increased markedly with decreasing solvent nucleophilicity can be explained by extended lifetimes of the cationic intermediate in weakly nucleophilic solvents. The yields of **9a-c** are similar to the fraction of **8a-c** formed after vicinal hydride shifts (*vide supra*) in each solvent, indicating that 1,2- and 1,3-type hydride shifts occur at comparable rates in the 4-homoadamantyl cation. The exclusive formation of the *exo*-isomer is presumably due to greater steric hindrance of the endo face of the 2-homoadamantyl cation. Similar face selectivity has been observed for the reduction of 2-homoadamantanone with lithium aluminum hydride or sodium borohydride (*exo*-OH:*endo*-OH = 0:100[20] and 5:95,[21] respectively).

2,4-Elimination. Different stereochemistries are expected for 1,3-type elimination to form 2,4-dehydrohomoadamantane (**11**), depending on whether H-2 is abstracted by tightly paired tosylate anion or solvent molecule. *endo*-H-2 should be abstracted selectively in

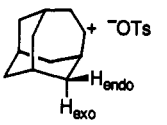

the former case, whereas in the latter case the abstraction of *exo*-H-2 would be favored by steric reasons. Although the present study does not definitively distinguish between the two possibilities, the latter mechanism seems more reasonable by the following reason. The fraction of **11** formed after vicinal hydride shifts is estimated by the amounts of label at positions other than C-3 and C-4: 1.3% (MeOH), 6.2% (AcOH), and 6.5% (TFE). These numbers are very close to those observed for 4-substituted products **8a-c** in each solvent, 1.4% (MeOH), 6.4% (AcOH), and 7.8% (TFE), indicating that **11** and **8a-c** are formed at essentially the same ion-pair stage. This result contrasts with that for 4-homoadamantene (**10**). As discussed earlier, the formation of **10**, in which the tosylate ion acts as the effective base, is accompanied by much smaller degrees of vicinal hydride shifts.

Experimental Section

Melting points are uncorrected. IR spectra were recorded on a Perkin–Elmer Model 1600 spectrophotometer. NMR spectra were obtained with a JEOL GSX270 instrument (^{1}H, 270 MHz; ^{13}C, 67.8 MHz) and reported in ppm (δ) from TMS. High-resolution mass analyses were perfomed with a JEOL JMS-HX110 mass spectrometer using electron impact ionization. Elemental analyses were performed by the Microanalytical Center, Kyoto University, Kyoto. Gas chromatographic analyses were conducted on a Hitachi 163 instrument equipped with a flame ionization detector and Hitachi Model D-2500 integrator using a PEG-20M column (3 mm × 2 m).

Reagents were of reagent-grade quality except when otherwise noted. Acetic acid was distilled in the presence of 3% acetic anhydride through a 30-cm Dewar column and stored with 1% acetic anhydride. Methanol was refluxed over sodium methoxide and distilled. 2,2,2-Trifluoroethanol was distilled in the presence of P_2O_5 through a 30-cm Dewar column. Ethanol was refluxed

(19) Nordlander, J. E.; Owuor, P. O.; Cabral, D. J.; Haky, J. E. *J. Am. Chem. Soc.* **1982**, *104*, 201.

(20) Yamaguchi, R.; Katsushima, T.; Kawanishi, M. *Bull. Chem. Soc. Jpn.* **1975**, *48*, 2328.

(21) Murray, R. K., Jr.; Babiak, K. A.; Morgan, T. K., Jr. *J. Org. Chem.* **1975**, *40*, 2463.

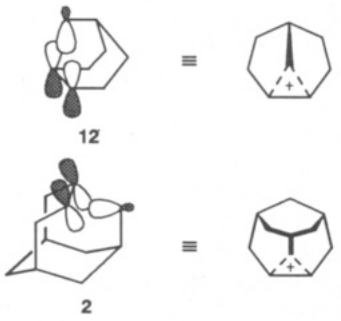

12

2

son[15] for the bicyclo[3.2.2]non-2-yl cation to explain the difficulty in attaining a σ-bridged structure.

Relative Rates of Wagner–Meerwein Rearrangement and Vicinal Hydride Shift. If the absence of frontside–backside stereospecificity with respect to the leaving group is assumed for both methylene and hydride migration, a diagram involving all the possible transformations among labeled 4-homoadamantyl cations $\mathbf{I}_n$ (n = 1–11) can be drawn as Scheme II.

The major distribution of the label at C-3 and C-4, but not at C-3 and C-6, with approximately equal populations clearly demonstrates predominant Wagner–Meerwein rearrangement (k_w) over 5,4-hydride shift (k_h). The formation of 4-substituted products **8a-c** labeled at positions other than C-3 or C-4 requires at least one hydride shift. The low total yields of such products, 1.4% (MeOH), 6.4% (AcOH),[16] and 7.8% (TFE), reflect the sluggishness of hydride shift compared to product formation. In particular, the negligible yields of **8a-c** labeled at C-7, -9, and -10, for which a second hydride shift is required, indicate that only the first hydride shift is significant. Further hydride shifts can then be ignored, thereby allowing simplification of the mechanistic model as illustrated in Scheme III.[17] $\mathbf{R}_n$ and $\mathbf{P}_n$ represent, respectively, the tosylate **7** and the 4-substituted product **8** labeled at the nth carbon. Rate constants k_i, k_{-i}, and k_p correspond to ionization, ion pair return, and product formation, respectively.

Steady-state treatment with respect to $\mathbf{I}_3$ and $\mathbf{I}_4$ results in the following rate expressions for tosylate consumption and product distribution

$$[\mathbf{R}_3] + [\mathbf{R}_4] = C_0 \exp\left(-\frac{k_i(k_p + k_h)}{k_{-i} + k_p + k_h}t\right) \quad (3)$$

$$[\mathbf{R}_3] - [\mathbf{R}_4] = C_0 \exp\left(-\frac{k_i(k_p + 2k_w + k_h)}{k_{-i} + k_p + 2k_w + k_h}t\right) \quad (4)$$

$$([\mathbf{P}_3] + [\mathbf{P}_4])_{t=\infty} = \frac{k_p}{k_p + k_h}C_0 \quad (5)$$

$$([\mathbf{P}_3] - [\mathbf{P}_4])_{t=\infty} = \frac{k_p}{k_p + 2k_w + k_h}C_0 \quad (6)$$

where C_0 is the initial concentration of the substrate [3-^{13}C]-**7**. Equations 5 and 6 afford expressions for the rates of Wagner–Meerwein rearrangement and vicinal hydride shift relative to solvent capture:

$$k_h/k_p = C_0/([\mathbf{P}_3] + [\mathbf{P}_4])_{t=\infty} - 1 \quad (7)$$

$$k_w/k_p = 0.5[C_0/([\mathbf{P}_3] - [\mathbf{P}_4])_{t=\infty} - (k_h/k_p) - 1] \quad (8)$$

From the fraction of **8a-c** labeled at C-3 and C-4 (Table IV), values for these rate ratios were calculated as listed in Table VII. This result allows evaluation of the rate of Wagner–Meerwein rearrangement relative to vicinal hydride shift: k_w/k_h = 340 ± 140 (MeOH), 140 ± 20 (AcOH), and 760 ± 340 (TFE).[18]

Ion Pair Return. The rates of ionization (k_i) and ion pair return (k_{-i}) in eqs 3 and 4 are related to two phenomenological rate constants, k_1 and k_{sc}.

$$k_1 = \frac{k_i(k_p + k_h)}{k_{-i} + k_p + k_h} \quad (9)$$

$$k_{sc} = \frac{k_i(k_p + 2k_w + k_h)}{k_{-i} + k_p + 2k_w + k_h} \quad (10)$$

The rate of tosylate scrambling, k_{sc}, can be derived from eq 4 using the data from acetolysis of [3-^{13}C]-**7** over 1.0 half-life (141 min). The recovered tosylate had retained 54.1 ± 0.5% label at C-3, and 44.1 ± 0.5% of the label was found at C-4. This result, which corresponds to k_{sc} = (2.72 ± 0.06) × 10^{-4} s^{-1}, indicates involvement of appreciable ion pair return through the Wagner–Meerwein process.

With this value for k_{sc} and the values for k_1, k_w/k_p, and k_h/k_p (Tables I and VII), eqs 9 and 10 are solved simultaneously with respect to k_1 and k_{-i}/k_p, yielding k_i = 3.1 × 10^{-4} s^{-1} and k_{-i}/k_p = 3.0. The fractional conversion

Scheme II

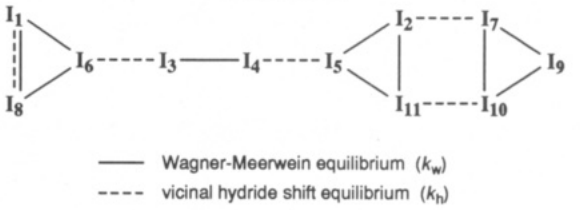

Scheme III

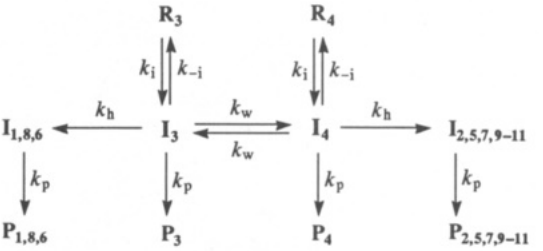

Table VII. Rate Constants of the Wagner–Meerwein Rearrangement (k_w) and 5,4-Hydride Shift (k_h) Relative to Solvent Capture (k_p) for the 4-Homoadamantyl Cation at 40 °C

solvent	k_w/k_p[a]	k_h/k_p
MeOH	4.1 ± 0.2	0.014 ± 0.005
AcOH	9.7 ± 0.8	0.068 ± 0.006
TFE	66 ± 33	0.085 ± 0.006

[a] See ref 18.

(15) Berson, J. A.; Luibrand, R. T.; Kundu, N. G.; Morris, D. G. *J. Am. Chem. Soc.* **1971**, *93*, 3075.

(16) Nordlander[4] reported that 18.6% of **8b** was formed with hydride shift in the acetolysis of [4-^{2}H]-**7**. As he pointed out, however, this number is an overestimation due to a large isotope effect by deuterium.

(17) The rate constant k_h as defined by Scheme III corresponds to half of that used in the kinetic treatment by Nordlander.[4]

(18) The errors in k_w/k_p and k_w/k_h are relatively large for TFE, since the small difference between $[\mathbf{P}_3]$ and $[\mathbf{P}_4]$ is amplified in eq 8.

1279, 1159, 1124 cm^{-1}. Anal. Calcd for $C_{13}H_{19}F_3O$: C, 62.89; H, 7.71; F, 22.96; Found: C, 62.68; H, 7.90; F, 23.22. **9c**: colorless liquid; ^{1}H NMR ($CDCl_3$) δ 3.78 (m, 2 H), 3.30 (m, 1 H), 2.2–1.2 (m, 16 H); IR (liquid film) 2906, 1278, 1157, 1122 cm^{-1}. HRMS calcd for $C_{13}H_{19}F_3O$ 248.1388, found 248.1403. Analysis for C gave a number slightly greater than calculated, since it was difficult to remove the solvent completely owing to high volatility. Anal. Calcd for $C_{13}H_{19}F_3O$: C, 62.89; H, 7.71. Found: C, 63.90; H, 7.84. The ^{13}C NMR spectral data for **8c** and **9c** are listed in Table III.

Quantitative ^{13}C NMR Analysis. The distribution of the ^{13}C label in the solvolysis products was determined from ^{13}C NMR spectra measured for undegassed $CDCl_3$ solutions in the presence of a relaxation reagent, $Fe(acac)_3$ (0.05 M).[10] The influence of the nuclear Overhauser enhancements was eliminated by employing the gated decoupling method. In order to ensure the accuracy of the signal intensity, FID signals were collected with a pulse interval of 3.0 s, which is longer than five times the longest relaxation times (T_1) shown by 4-homoadamantyl acetate. Spectra were recorded with a digital resolution of 0.35–0.52 Hz using an exponential multiplication corresponding to the line broadening of 1.0 Hz. Signals obtained by this procedure consisted of more than 20 points. Basically, signal intensities were obtained by digital integration using the NMR instrument. When two peaks overlap partially, they were resolved by the cut-and-weigh method. Repeated measurements showed that the precision was ca. ±0.5% for C-3 and C-4 and ca. ±0.2% for other carbons.

Kinetic Measurements. The methods for kinetic measurements were described previously.[25] All measurements were conducted in the presence of 0.025 M 2,6-lutidine with substrate concentrations of (1–2) × 10^{-2} M (titrimetric method) or (2–20) × 10^{-4} M (conductimetric method). The first-order rate constants were calculated by the least-squares method.

Acknowledgment. We thank Prof. Ryohei Yamaguchi for providing us with *exo*-2-hydroxy-4-homoadamantene.

Supplementary Material Available: ^{1}H and ^{13}C NMR spectra of **9a** and **9c** (4 pages). This material is contained in libraries on microfiche, immediately follows this article in the microfilm version of the journal, and can be ordered from the ACS; see any current masthead page for ordering information.

(25) Takeuchi, K.; Ikai, K.; Shibata, T.; Tsugeno, A. *J. Org. Chem.* 1988, *53*, 2852.

Notes

Synthesis of 3-Vinylpyrrole

Roberta Settambolo,† Raffaello Lazzaroni,‡ Tommaso Messeri,‡ Michele Mazzetti,‡ and Piero Salvadori*,‡

Istituto di Chimica Quantistica ed Energetica Molecolare del CNR, and Centro di Studio del CNR per le Macromolecole Stereordinate ed Otticamente Attive, Dipartamento di Chimica e Chimica Industirale, Via Risorgimento 35, I-56126 Pisa, Italy

Received June 2, 1993

In recent years, 3-alkylpyrroles have been investigated as starting monomers for the preparation of organic conducting materials,[1] as well as precursors in porphyrin chemistry.[2] At present, simple 3-alkenylpyrroles are the subject of considerable interest. These compounds, reactive both at the exocyclic double bond and at positions 2 and 5 of the pyrrole ring, represent interesting bifunctional monomers for the synthesis of polypyrroles.[3] It is surprising that, although an ab initio molecular orbital study of the simplest member of this class, 3-vinylpyrrole, has been reported,[4] this compound has never been synthesized. Its supposed inaccessibility and/or instability is a possible explanation.[5] We report here a simple general method which leads in five steps from pyrrole to 3-ethenylpyrroles with good yield of isolated, pure product. The 3-acyl-1-tosylpyrroles, easily obtained by the procedure of Kakushima et al.,[6] were successfully used as starting material to prepare 3-vinylpyrrole **8a** and some related compounds **8b–d** (Scheme I), previously unreported in the literature.

Results and Discussion

The synthetic sequence used is shown in Scheme I. Pyrrole (1) was treated with tosyl chloride under catalytic phase-transfer conditions to give 1-tosylpyrrole (2) in high yield.[7,8] Then **2** was acetylated to afford 3-acetyl-1-tosylpyrrole (**3a**)[9] in quantitative yield using acetic anhydride and $AlCl_3$, according to the experimental conditions described by Kakushima[6] et al. for 3-acetyl-1-phenylsulfonyl)pyrrole. The partial reduction of **3a** to 3-(1-hydroxyethyl) derivative **4a** is a crucial step in the reaction sequence. Whereas some methods for the reductive deoxygenation of 3-acyl-1-(phenylsulfonyl)pyrroles

Scheme I

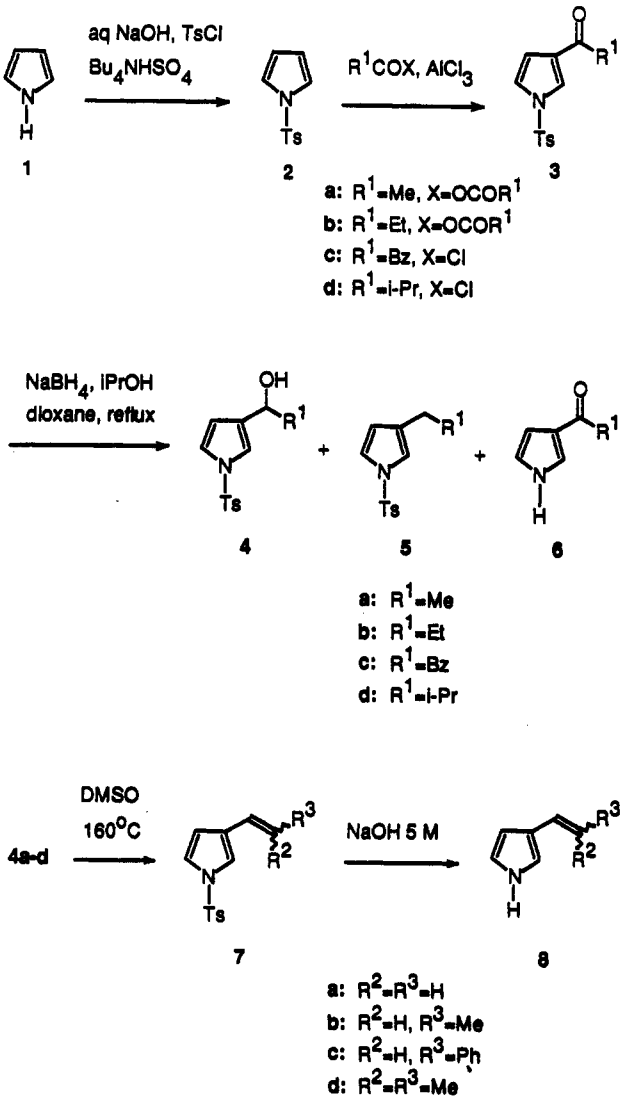

to 3-alkyl-1-(phenylsulfonyl)pyrroles have been described in the literature,[7,10,11] the preparation of 3-(1-hydroxyalkyl)pyrroles from acylic precursors has not been developed. After several attempts, we found that the treatment of **3a** with $NaBH_4$ and 2-propanol in boiling dioxane (molar ratio **3a**/$NaBH_4$/2-propanol = 1:0.5:1) gives the best yield of the hydroxyl derivative **4a** (Table I). When less 2-propanol was present, no reaction was observed. On the other hand, upon carrying out the reaction in pure 2-propanol, significant deprotection of the nitrogen atom occurred and the resulting N-unsubstituted 3-acetylpyrrole was recovered. The reaction is not completely chemoselective, affording **4a** along with the corresponding 3-ethyl-1-tosylpyrrole (**5a**) (20%) and traces of detosylated acyl derivative **6a**. The isolation of **4a**, as a pure yellow oil (70% yield), was accomplished by liquid chromatography on a silica gel column, eluting with chloroform–

† Istituto di Chimica Quantistica ed Energetica Molecolare del CNR.
‡ Centro di Studio del CNR per le Macromolecole Stereordinate ed Otticamente Attive.

(1) Inagaki, T.; Hunter, M.; Yang, X. Q.; Skotheim, T. A.; Okamoto, Y. *J. Chem. Soc., Chem. Commun.* **1988**, 126.
(2) Smith, K. M.; Bisset, G. M. F. *J. Org. Chem.* **1979**, *44*, 2077.
(3) Kamogawa, H.; Nakata, T.; Ohori, S.; Komatsu, S. *Bull. Chem. Soc. Jpn.* **1991**, *64*, 1066.
(4) Kao, J.; Hinde, A. L.; Radom, L. *Nouv. J. Chim.* **1979**, *3*, 473.
(5) (a) Jones, R. A.; Marriott, M. T. P.; Rosenthal, W. P.; Arques, J. S. *J. Org. Chem.* **1980**, *45*, 4515. (b) Hosmane, R. S.; Hiremath, S. P.; Schneller, S. W. *J. Chem. Soc., Perkin Trans. 1*, **1973**, 2450.
(6) Kakushima, M.; Hamel, P.; Frenette, R.; Rokach, J. *J. Org. Chem.* **1983**, *48*, 3214.
(7) Anderson, H. J.; Loader, C. E.; Xu, R. X.; Lê, N.; Gogan, N. J.; McDonald, R.; Edwards, L. G. *Can. J. Chem.* **1985**, *63*, 896.
(8) Papadopoulos, E. P.; Haidar, N. F. *Tetrahedron Lett.* **1968**, *14*, 1721.
(9) Muratake, H.; Natsume, M. *Heterocycles* **1990**, *31*, 683.
(10) Ketcha, D. M.; Carpenter, K. P.; Atkinson, S. T.; Rajagopalan, H. R. *Synth. Commun.* **1990**, *20*, 1647.
(11) Greenhouse, R.; Ramirez, C.; Muchowski, J. M. *J. Org. Chem.* **1985**, *50*, 2961.

0022-3263/93/1958-7899$04.00/0

Table I. Reduction of 3-Acyl-1-Tosylpyrroles 3a–d to 3-(1-Hydroxyalkyl)-1-tosylpyrroles 4a–d with $NaBH_4$ and 2-Propanol in Dioxane at Reflux

starting material		reaction	product		
entry	compd	time, h	compd	yield,[a] %	purification process (CC[b])
1	3a	6.5	4a	70	oil; $CHCl_3$–EtOAc (70:30)
2	3b	7.0	4b	67	oil; CCl_4–Et_2O (1:1)
3	3c	4.0	4c	72	solid;[c] hexane–EtOAc (2:1)
4	3d	5.5	4d	48	oil; hexane–Et_2O (2:3)

[a] Yield of pure isolated product 4 based on 3. [b] CC = Column chromatography: the stationary phase was silica gel. [c] Mp 90–92 °C.

ethyl acetate (70:30). Several attempts at the dehydration of 4a under a variety of experimental conditions[12] were unsuccessful, leading to decomposition or oligomer formation. Finally, 3-vinyl-1-tosylpyrrole (7a) was obtained by heating 4a under neutral conditions with anhydrous DMSO at 160 °C, following the procedure described by Traynelis et al. for the dehydration of benzylic alcohols.[13] The crude product was chromatographed (SiO_2; $CHCl_3$–hexane = 1:1) to obtain 7a as a colorless solid in 94% yield (Table II). In order to remove the tosyl group, 7a was submitted to heat treatment with NaOH in 2-propanol/water. The result was 3-vinylpyrrole (8a), obtained as a pale yellow oil (82% yield, Table III) by distillation at reduced pressure. Contrary to what was previously supposed,[5] 8a is stable enough to be distilled without any decomposition, easily handled at room temperature, and perfectly stable for long periods at 0 °C.

The same reaction sequence afforded 3-(1-propenyl)-pyrrole (8b), 3-(2-phenylethenyl)pyrrole (8c), and 3-(2-methyl-1-propenyl)pyrrole (8d) in good overall yield of isolated pure product (Tables I–III), respectively, from 3b–d. As observed for 3-vinylpyrrole, the compounds 8b–d are stable at 0 °C.

In one case (entry 2 in Table III), the addition of diphenylamine as a polymerization inhibitor was necessary in order to prevent the formation of oligomers during the basic hydrolysis. All the newly synthesized compounds 3b–d, 4a–d, 7a–d, and 8a–d were characterized by ^1H NMR, MS, and elemental analysis.

3-Alkyl-1-tosylpyrrole byproducts arising from the reduction step undergo no detosylation under the experimental conditions adopted. As a consequence they can be easily eliminated during the purification of the final product.

It must be noted that the sequence used for the preparation of 8a–d cannot be varied. Attempts to carry out the reduction of N-unsubstituted 3-acetylpyrrole[6] (6a) in boiling dioxane/2-propanol/$NaBH_4$ were unsuccessful, with unreacted starting substrate being recovered. On the other hand, the N-tosylated alcohols decomposed to some extent under the basic hydrolysis conditions used in the detosylation step; therefore the tosyl group must be removed after the dehydration step. This clearly indicates that the partial reduction of the 3-acyl-1-tosylpyrroles 3 to the corresponding alcohols 4 is the key step in the synthesis of the 3-ethenylpyrroles 8. The reduction of both 3-(phenylacetyl)-1-tosylpyrrole (3c) and 3-(isobutyryl)-1-tosylpyrrole (3d) affords only traces of the alkyl derivatives 5c and 5d. In these cases, 3-(phenylacetyl)-pyrrole (6c) and 3-(isobutyryl)pyrrole (6d), arising from detosylation of 3c and 3d, were recovered (15 and 28% of isolated product, respectively), along with the desired alcohols 4c and 4d.

(12) (a) Hoffman, R. V.; Bishop, R. D.; Fitch, P. M.; Hardenstein, R. *J. Org. Chem.* **1980**, *45*, 917. (b) Giner, J. L.; Margot, C.; Djerassi, C. *J. Org. Chem.* **1989**, *54*, 369. (c) Botteghi, C.; Caccia, G.; Gladiali, S.; Tatone, D. *Synth. Commun.* **1979**, *9*, 69.

(13) Traynelis, V. J.; Hergenrother, W. L.; Livingston, J. R.; Valicenti, J. A. *J. Org. Chem.* **1962**, *27*, 2377.

Conclusion

A suitable synthetic route to the 3-ethenylpyrroles has been developed, starting from readily available 3-acetyl-1-tosylpyrroles. The expected p-toluenesulfonic acid is the main byproduct of the reaction sequence, which employs inexpensive reagents and provides pure products after a simple purification process. This easy accessibility to the 3-ethenylpyrroles makes these compounds a convenient source of other 3-substituted pyrrole derivatives. Among the synthesized products, 3-vinylpyrrole 8a constitutes the most interesting substrate for experimental and theoretical investigations.

Experimental Section

All reagents were of commercial quality. Silica gel (70–230 mesh) was purchased from Merck. DMSO was refluxed and then distilled over sodium hydroxide pellets. The NH_3-saturated eluents used in the column chromatography were obtained by bubbling gaseous NH_3 into organic mixture at 0 °C. Melting points were taken using a Reichart Thermovar apparatus and were uncorrected. Microanalyses were performed at Laboratorio di Microanalisi, Istituto di Chimica Organica, Facoltà di Farmacia, Università di Pisa. ^1H NMR spectra were recorded on a Varian Gemini-200 (200 MHz) or VXR-300 (300 MHz) spectrometers with TMS as internal standard and $CDCl_3$ as the solvent. Electron impact mass spectra were recorded on a Perkin Elmer Q-Mass 910 mass spectrometer interfaced with a Perkin Elmer 8500 gas chromatograph. 1-Tosylpyrrole (2)[7,8] and 3-acetyl-1-tosylpyrrole (3a)[6,9] were synthesized as described in the literature.

3-Acyl-1-tosylpyrroles. General Procedure. 3-Propionyl-1-tosylpyrrole (3b). The procedure of Kakushima[6] et al. was used. To a suspension of anhydrous $AlCl_3$ (46.4 g, 0.348 mol) in 750 mL of dichloromethane at 25 °C was added slowly propionic anhydride (23.0 g, 0.177 mol) and the resulting mixture was stirred for 15 min. A solution of 2 (12.0 g, 0.054 mol) in 150 mL of dichloromethane was added dropwise, and the mixture was stirred at 25 °C for 2 h. The reaction was quenched with ice and water, and the aqueous layer was extracted with additional dichloromethane (3 × 200 mL). The combined organic layers were treated with saturated $NaHCO_3$, washed with brine, dried (Na_2SO_4), and evaporated in vacuo to give a red solid. Crystallization from ether gave 3b (12.5 g, 0.045 mol, 84%) as colorless needles: mp 67–69 °C; ^1H NMR δ 7.80 (d, 2 H, J = 8.26 Hz), 7.74 (dd, 1 H, J = 1.68, 2.16 Hz, H2), 7.34 (d, 2 H, J = 8.26 Hz), 7.14 (dd, 1 H, J = 2.16, 3.31 Hz, H5), 6.68 (dd, 1 H, J = 1.68, 3.31 Hz, H4), 2.76 (q, 2 H, J = 7.34 Hz, CH_2), 2.42 (s, 3 H), 1.15 (t, 3 H, J = 7.34 Hz, CH_3); MS m/e 277 (M^+, 2.0), 248 (36.5), 155 (43.8), 91 (100), 65 (32.1), 39 (67.3). Anal. Calcd for $C_{14}H_{15}NO_3S$: C, 60.63; H, 5.45; N, 5.05. Found: C, 60.81; H, 5.53; N, 4.95.

3-(Phenylacetyl)-1-tosylpyrrole (3c). Prepared according to the general procedure except that phenylacetyl chloride (21.04 g, 0.136 mol), $AlCl_3$ (18.0 g, 0.135 mol), and 2 (10 g, 0.045 mol) were used. Yield 12.16 g (0.036 mol, 80%) of pure 3c as a yellow-orange solid (SiO_2; hexane–EtOAc = 6:4): mp 84.5–87.5 °C; ^1H NMR δ 7.78–7.75 (m, 2 H), 7.34–7.23 (m, 8 H), 7.11 (dd, 1 H, J = 2.08, 3.42 Hz, H5), 6.69 (dd, 1 H, J = 1.71, 3.42 Hz, H4), 4.02 (s, 2 H, CH_2), 2.42 (s, 3 H); MS m/e 248 (M^+ – 91, 100), 155 (56.4), 91 (66.0), 65 (21.7), 39 (30.6). Anal. Calcd for $C_{18}H_{17}NO_3S$: C, 67.24; H, 5.05; N, 4.13. Found: C, 67.10; H, 5.02; N, 4.31.

3-(Isobutyryl)-1-tosylpyrrole (3d). Prepared according to the general procedure except that isobutyryl chloride (13.23 g, 0.124 mol), $AlCl_3$ (18.10 g, 0.135 mol), and 2 (25.00 g, 0.113 mol) were used. Yield 30.8 g (0.106 mol, 94%) of pure 3d as a colorless oil (SiO_2; hexane–Et_2O = 6:4): ^1H NMR δ 7.80 (d, 2 H, J = 8.26 Hz), 7.75 (dd, 1 H, J = 1.68, 2.13 Hz, H2), 7.34 (d, 2 H, J = 8.26 Hz), 7.14 (dd, 1 H, J = 2.13, 3.32 Hz, H5), 6.69 (dd, 1 H, J = 1.68,